FACTA UNIVERSITATIS
Series: **Mechanical Engineering**
https://doi.org/10.22190/FUME210207007J

Original scientific paper

DETECTION OF NONLOCAL CALIBRATION PARAMETERS AND RANGE INTERACTION FOR DYNAMICS OF FGM POROUS NANOBEAMS UNDER ELECTRO-MECHANICAL LOADS

Piotr Jankowski

Faculty of Mechanical Engineering, Bialystok University of Technology, Poland

Abstract. *The present investigation examines the range of effect of nonlocal parameters on dynamic behavior of a smart beam-like nanostructure modeled as sandwich functionally graded porous nanobeam with piezoelectric layers. Therefore, the study is concentrated on determining length of the structure for which nonlocal effects are observed for vibration of nanobeam under in-plane electro-mechanical forces. The nanobeam-based NEMS device model is obtained based on assumptions of the nonlocal strain gradient theory in conjunction with Reddy higher-order shear deformation theory. The investigation present differences in obtained results for nanostructure's free vibration based on classical and nonlocal assumptions. To study range of application of nonlocal parameters for different length of simply supported nanobeam, defined eigenvalue problem is solved in view of variation of length to thickness ratio, distribution of material properties, as well as electro-mechanical loads. What is more, the study attempts to determine and calibrate values of size-dependent coefficients based on expected natural frequencies, material properties, and applied loads. The results are completed with extensive discussion on the dependence of nonlocal parameters on nanobeam's dynamic response, thus may be an important step forward to extend understanding of ultra-small structure's behavior.*

Key words: *Nanobeam, FGM, Porosity, Piezoelectric effect, Free vibration, Detected nonlocal parameters*

1. INTRODUCTION

Nanoelectromechanical systems (NEMS) are modern devices that employ ultra-small structures in form of beams, plates, and shells which are powered by electrical circuits

*__Received:__ February 07, 2022 / Accepted February 26, 2022
Corresponding author: Piotr Jankowski
Faculty of Mechanical Engineering, Bialystok University of Technology, Wiejska 45C, 15-351 Bialystok, Poland
E-mail: p.jankowski@doktoranci.pb.edu.pl

[1]. Due to extremely small size of the structure, these devices experience unique properties and characteristics. This special kind of structure found applications in various areas, such as logic switches, sensors, actuators, and energy harvesting [2-4]. Ultra-small devices operation may be based, inter alia, on electromagnetic [5], piezoelectric [6], and thermo-electric [7] phenomena. What is more, operations principle for diverse small-scaled devices is based on their buckling and vibration characteristics [8].

In view of ultra-small dimensions of the structure, the size-dependent characteristic is fundamental in modelling of mechanical behavior of nano- and micro-sized elements [9]. There are diverse approaches to study small-scaled structures, including molecular dynamics [10] as well as continuum-based nonlocal theories. The latter characterizes lower computational effort for very complex ultra-small systems, and therefore gained much interest [11]. It should be noted, due to size-dependent phenomena, the classical continuum-based theories are insufficient to accurately describe mechanical behavior of ultra-small structures. Among advanced continuum-based nonlocal theories, that capture size-dependent effects in micro- and nanostructures, one can distinguish the couple stress theory [12-14], the modified couple stress theory [15], Mindlin's strain gradient theory [16,17], the modified strain gradient theory [18], Gurtin-Murdoch surface elasticity [19], the nonlocal elasticity [20-24], the stress-driven nonlocal integral elasticity [25] and a higher-order nonlocal elasticity and strain gradient theory [26]. Among these, the strain-gradient-based ones are established on assumption that ultra-small structures' mechanical behavior depends on classical strains and higher-order gradient of strains. On the other hand, the stress-based theories indicate that the key role in size-dependent characteristics has classical stresses and higher-order gradients of stresses Two entirely different responses, such as stiffness softening and hardening effects, has been seen in nanostructures mechanical behavior [27]. Therefore, it has become an important issue to combine both phenomena in one refined theory [26,28].

Diverse methods and approaches were used in modelling and analyzing nanostructures [29-41], nevertheless in the current literature survey is focused on dynamics of beam-like nanostructures. Wang and Varadan [42] presented effect of Eringen's nonlocal parameter on frequency of both single-walled and double-walled carbon nanotubes based on Euler-Bernoulli beam theory. Reddy [43] compared results obtained for diverse beam models for bending, buckling and free vibration of simply supported nanobeams considering nonlocal elasticity of Eringen. Wang et al. [44] studied influence of small-scale parameter from Eringen's nonlocal theory and diverse length to diameter ratio on vibrations of single-walled nanotubes modelled by Timoshenko beam theory with diverse boundary conditions (BCs). Aydogdu [45] used Eringen's nonlocal elasticity to study axial vibration of nanorods with clamped-clamped and clamped-free BCs based on Euler-Bernoulli model assumptions. Roque et al. [46] employed RBF meshless numerical formulation to study bending, buckling, and free vibration of Timoshenko nanobeams using nonlocal elasticity theory. Li et al. [47] conducted a study on transverse vibrations of simply supported Euler-Bernoulli nanobeam under axial mechanical load. Thai [48], and then Thai and Vo [49] presented a closed-form solution for deflection, buckling, and vibration of Eringen's nanobeam under transverse loads modelled by diverse refined beam theories. Ke et al. [50] investigated piezoelectric effect on nonlinear vibration of Timoshenko nanobeam with various BCs using the Differential Quadrature Method (DQM). Eltaher et al. [51] used Euler-Bernoulli beam assumptions and a finite element formulation to study eigenfrequencies of functionally graded (FG)

nanobeam based on Eringen's nonlocal theory. Berrabah et al. [52] analytically solved bending, buckling and vibration problems of Eringen's nanobeam modelled via various theories. Şimşek [53] compared nonlinear to linear frequencies obtained for Euler-Bernoulli nanobeam with various boundary conditions based on a nonlocal elasticity. Rahmani and Pedram [54] presented analytical solution for natural frequencies of functionally graded nanobeam according to Timoshenko beam and Eringen's nonlocal theories. Nejad and Hadi [55] analyzed impact of bi-directional functionally graded material properties on Eringen's nanobeam vibrational response using the Generalized Differential Quadrature Method (GDQM). Beni [56] discussed impact of piezoelectric phenomenon on nonlinear vibration and bending characteristics of Euler-Bernoulli nanobeam using the couple stress theory. Arefi and Zenkour [57] discussed effect of electric field on vibration and bending of nanobeam with piezomagnetic layers resting on Winkler-Pasternak foundation based on Timoshenko beam model assumptions and Eringen's nonlocal elasticity. Lu et al. [58] used the nonlocal strain gradient theory to perform analysis of nanobeams free vibration based on the sinusoidal shear deformation theory. Liu et al. [59] examined vibration response of visco-elastic functionally graded porous Timoshenko nanobeam with magneto-electro-elastic coupling effect for different boundary conditions. Thai et al. [60] analytically solved deflection and vibration problems of Eringen's nanobeams subjected to uniformly distributed load. Karami and Janghorban [61] proposed novel higher-order shear deformation beam theory and studied natural vibration of functionally graded nanobeam using nonlocal strain gradient theory. Liu et al. [62] utilized Galerkin approach to study nonlinear vibration of functionally graded sandwich nanobeam with diverse boundary conditions based on the nonlocal strain gradient theory and Euler-Bernoulli model. Jankowski et al. [63,64] presented analytical and numerical approaches to study vibrational behavior of FG and sandwich FG with piezoelectric layers nanobeams based on Reddy third-order shear deformation theory and the nonlocal strain gradient theory. Nasr et al. [65] studied effect two-parameter foundation and thermoelastic phenomenon on deflection and vibration nanobeam based on Euler-Bernoulli beam assumptions and Eringen's nonlocal elasticity.

1.1 Novelty of the Present Study

Based on the best author's knowledge and presented literature survey there is a lack of investigation focused on the range of nonlocal parameters interaction on dynamic response of functionally graded porous beam-like nanostructures, with simply supported edges, under in-plane electromechanical forces. Achieved nano-actuator model based on the nonlocal strain gradient theory in conjunction with the Reddy third-order shear deformation theory enables a wide spectrum to analyze nanostructures dynamic response in view of nonlocal parameters as well as geometrical and material properties. The study ensures different point of view to the analysis of vibrational response of nanobeams. In contrast to previous papers, the present investigation is focused on an influence range of nonlocal parameters on dynamic behavior of nanostructure in view of material and geometrical properties together with an applied electromechanical load. The investigation considers length of the nanostructure at which the nonlocal phenomena have crucial influence on its vibrational response. In accordance with this objective, the study displays differences in results obtained based on classical and nonlocal assumptions. What is more, the present study together with solution methodology provides a possibility to

estimate values of small-scale parameters depending on expected fundamental frequencies, assumed, or predicted material properties along with mechanical and electrical forces acting in NEMS devices. The presented approach could be an important tool in better understanding NEMS structures and consequently, may avoid some of cost-consuming and complex material characterization processes, especially for NEMS devices in engineering applications.

2. Higher-Order Nonlocal Elasticity and Strain Gradient Theory

A higher-order nonlocal elasticity and strain gradient theory called as the nonlocal strain gradient theory [26] is a novel hybrid refined theory that enables consider both stiffnesses softening and hardening effects in the nanostructure. Thus, such an approach allows taking advantage of Eringen's nonlocal theory and Mindlin's strain gradient theory from a single point of view [66]. According to assumptions of the nonlocal strain gradient theory, the total stress tensor is presented in the form:

$$\sigma = \bar{\sigma} - \nabla \bar{\sigma}^{(1)} \tag{1}$$

where $\bar{\sigma}$ refers to classical stresses (work conjugate of classical strains) and $\bar{\sigma}^{(1)}$ to higher-order stresses (work conjugate of gradients of strains). Used vector differential operator $\nabla = \boldsymbol{e_i}\partial/\partial \boldsymbol{x_i}$ is coupled with unit vector $\boldsymbol{e_i}$ and direction $\boldsymbol{x_i}$ of a nonlocal effect (gradient) in nanostructure. The classical and higher-order stress tensors are derived as:

$$\bar{\sigma} = \int_V \alpha_0(\boldsymbol{x}', \boldsymbol{x}, e_0 a)\boldsymbol{C} : \varepsilon' dV' \tag{2a}$$

$$\bar{\sigma}^{(1)} = \ell^2 \int_V \alpha_1(\boldsymbol{x}', \boldsymbol{x}, e_1 a)\boldsymbol{C} : \nabla\varepsilon' dV' \tag{2b}$$

where α_0 and α_1 represent principial and additional attenuation kernel functions to describe nonlocality effects in terms of the Euclidean distance between the point $\boldsymbol{x}$ and neighboring points $\boldsymbol{x'}$ in the domain V. Additionally, ℓ stands for the length scale parameter form the strain gradient theory, as well as e_0 and e_1 are nonlocal constants together with a represent internal characteristic length. Then, ε' is the Cartesian components of the strain tensor at point $\boldsymbol{x'}$, and $\boldsymbol{C}$ is the elastic modulus tensor of classical elasticity. A general form of constitutive equations in differential form may be obtained assuming that nonlocal attenuation kernel functions satisfy conditions proposed by Eringen [24] and applying linear differentiational operators on both sides of Eq. (1). The differential operator is in the form:

$$L_i = 1 - (e_i a)^2 \nabla^2 \quad \textit{for } i = 0,1 \tag{3}$$

The generalized nonlocal constitutive relations based on the higher-order nonlocal elasticity and strain gradient theory take the form:

$$[1-(e_1 a)^2\nabla^2][1-(e_0 a)^2\nabla^2]\sigma = [1-(e_1 a)^2\nabla^2]\boldsymbol{C} : \varepsilon - \ell^2[1-(e_0 a)^2\nabla^2]\boldsymbol{C} : \nabla^2\varepsilon \tag{4}$$

Where $\nabla^2 = \partial^2/\partial \boldsymbol{x}^2$ is one dimensional differential operator. Assuming $e_0 = e_1 = e$ the higher-order constitutive relations may be easily reduced to the lower-order nonlocal strain gradient model:

$$[1-(ea)^2\nabla^2]\sigma = [1-\ell^2\nabla^2]\boldsymbol{C}:\varepsilon \tag{5}$$

What is more, based on the present model, Eringen's nonlocal elasticity may be obtained assuming $\ell = 0$:

$$[1-(ea)^2\nabla^2]\sigma = \boldsymbol{C}:\varepsilon \tag{6}$$

From the other point of view, form of Mindlin's strain gradient theory may be achieved by taking $ea = 0$:

$$\sigma = [1-\ell^2\nabla^2]\boldsymbol{C}:\varepsilon \tag{7}$$

Finally, classical constitutive relations may be obtained while both nonlocal coefficients are assumed to be zero.

3. Material Properties and Piezoelectric Effect

3.1 Three-Layered FGM Nanobeam

In the study we consider composite nanobeam-like actuator model that consists of porous functionally graded nanobeam with thickness h and piezoelectric layers of thicknesses h_p. The total thickness of the nanostructure is assumed $H = h + h_p$, length L and unit width b. Between FGM core and piezoelectric face-sheets it is presumed ideal mechanical contact. To imitate environment impact in the NEMS device, the nanobeam is subjected to an electrical field with external voltage ϕ_0 and axial compressive/tensile mechanical in-plane forces $\hat{N}_{xx}$. The cross-section and coordinate system of sandwich nanobeam are presented in Fig. 1.

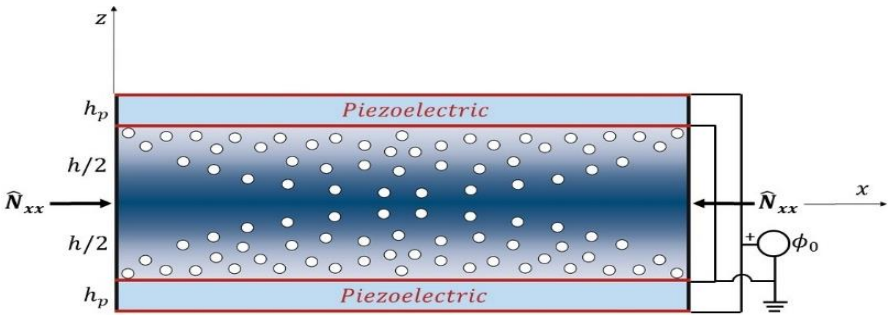

Fig. 1 Three-layered porous FGM nanobeam as a nanoactuator model

3.2 Functionally Graded Core

Elastic parameters of the functionally graded porous nanobeam core are given by:

$$C_{xx} = E(z,\Upsilon) \tag{8a}$$

$$C_{xz} = \frac{E(z,\Upsilon)}{2(1+\upsilon)} \tag{8b}$$

$E(z,\Upsilon)$ stands for Young's modulus of nanobeam core and $\Upsilon(z,\vartheta)$ is porosity distribution function. Young's modulus, as well as an FG porous structure mass density $\rho(z,\vartheta)$, vary in the thickness direction according to the power-law distribution. In the study, Poisson's ratio υ is assumed to be constant since its low volatility has negligible influence on mechanical behavior of the structure. Properties of functionally graded core are symmetric with respect to the midplane, and presented as:

$$E(z,\Upsilon) = [(E_c - E_m)V^{(n)}(z,g) + E_m][1 - \Upsilon(z,\vartheta)] \tag{9a}$$

$$\rho(z,\Upsilon) = [(\rho_c - \rho_m)V^{(n)}(z,g) + \rho_m][1 - \Upsilon(z,\vartheta)] \tag{9b}$$

Components of the functionally graded material generally consist of ceramic (E_c, ρ_c) and metallic (E_m, ρ_m) parts but can be replaced by other materials/nanomaterials with well-known experimental values of elastic/physical parameters. Properties of functionally graded core are assumed to be symmetric with respect to the midplane. The volume fraction function $V^{(n)}$ controls volatility of material distribution through the nanobeam core thickness, and is described as follows:

$$V^{(1)} = \left(\frac{z + \frac{h}{2}}{\frac{h}{2}} \right)^g \quad for\ z \in \left\langle -\frac{h}{2}, 0 \right\rangle \tag{10a}$$

$$V^{(2)} = \left(\frac{z - \frac{h}{2}}{-\frac{h}{2}} \right)^g \quad for\ z \in \left\langle 0, \frac{h}{2}, \right\rangle \tag{10b}$$

where g is the power-law index.

In the investigation, we consider three diverse symmetric to the midplane porosity distributions:

$$Type\ 1: \Upsilon(z,\vartheta) = \vartheta \cos\left(\frac{\pi z}{h}\right) \tag{11a}$$

$$Type\ 2: \Upsilon(z,\vartheta) = \begin{cases} \vartheta \cos\left[\pi\left(\frac{2z}{h} + \frac{1}{2}\right)\right] & for\ z \in \left\langle -\frac{h}{2}, 0 \right\rangle \\ \vartheta \cos\left[\pi\left(\frac{2z}{h} - \frac{1}{2}\right)\right] & for\ z \in \left\langle 0, \frac{h}{2}, \right\rangle \end{cases} \tag{11a}$$

$$Type\ 3: \Upsilon(z,\vartheta)=\begin{cases}\vartheta\cos\left[\pi\left(\dfrac{z}{h}+\dfrac{1}{2}\right)\right] & for\ z\in\left\langle-\dfrac{h}{2},0\right\rangle\\ \vartheta\cos\left[\pi\left(\dfrac{z}{h}-\dfrac{1}{2}\right)\right] & for\ z\in\left\langle 0,\dfrac{h}{2},\right\rangle\end{cases} \tag{11a}$$

where ϑ refers to averaged volume of voids in the structure called porosity coefficient. Distributions as well as volume of voids, together with variation of volume fraction function are shown in Fig. 2.

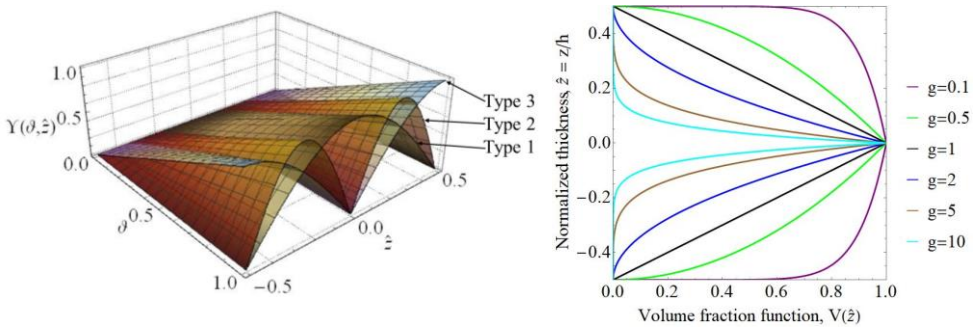

a) b)

Fig. 2 Material variation in functionally graded nanobeam core: a) porosity distribution and accumulation; b) volume fraction function

3.3 Piezoelectric Relations

The studied nanobeam is subjected to an electric field. Electric potential $\breve{\Phi}$ is presented as approximated combination of half-cosine and linear variation [67] satisfying Maxwell relations:

$$\breve{\Phi}(x,z,t)=-\cos\left(\frac{\pi z_p}{h_p}\right)\Phi(x,t)+\frac{2z_p}{h_p}\phi_0 \tag{12}$$

where z_p stands for variable that is measured from the geometrical center of the piezoelectric layers, $z_1 = z\text{-}h/2\text{-}h_p/2$ for top face-sheet and $z_2 = z\text{+}h/2\text{+}h_p/2$ for bottom face-sheet. Additionally, $\Phi(x,t)$ refers to variation of electric potential in longitudinal direction. Electric field components are achieved based on electric potential function:

$$E_x=-\frac{\partial\breve{\Phi}}{\partial x}=\cos\left(\frac{\pi z_p}{h_p}\right)\frac{\partial\Phi}{\partial x} \tag{13a}$$

$$E_z=-\frac{\partial\breve{\Phi}}{\partial z}=-\frac{\pi}{h_p}\sin\left(\frac{\pi z_p}{h_p}\right)\Phi-\frac{2}{h_p}\phi_0 \tag{13b}$$

4. Displacement Field and Constitutive Equations

Displacement vector components are described in the framework of Reddy third-order shear deformation theory [68]:

$$u_x\left(x,z,t\right)=u_0\left(x,t\right)+z\varphi_x\left(x,t\right)-c_1z^3\left(\varphi_x\left(x,t\right)+\frac{\partial w_0\left(x,t\right)}{\partial x}\right) \tag{14a}$$

$$u_z\left(x,z,t\right)=w_0\left(x,t\right) \tag{14b}$$

where u_0 and w_0 are axial and transverse displacements of material point on the midplane in an undeformed configuration, φ_x is rotation of a point on the centroidal axis x of the beam, and $c_1 = 4/(3H^2)$ for clarity of formulation. The strain-displacement relations are presented as linear and infinitesimal Green-Lagrange strain tensor:

$$\left\{\varepsilon^{(0)}{}_{xx},\varepsilon^{(1)}{}_{xx},\varepsilon^{(3)}{}_{xx}\right\}=\left\{\frac{\partial u_0}{\partial x},\frac{\partial\varphi_x}{\partial x},-c_1\left(\frac{\partial\varphi_x}{\partial x}+\frac{\partial^2w_0}{\partial x^2}\right)\right\} \tag{15a}$$

$$\left\{\gamma^{(0)}{}_{xz},\gamma^{(2)}{}_{xz}\right\}=\left\{\varphi_x+\frac{\partial w_0}{\partial x},-c_2\left(\varphi_x+\frac{\partial w_0}{\partial x}\right)\right\} \tag{15b}$$

where $c_2 = 3c_1$. Thus, the strains take the form:

$$\varepsilon_{xx}=\varepsilon^{(0)}{}_{xx}+z\varepsilon^{(1)}{}_{xx}+z^3\varepsilon^{(3)}{}_{xx} \tag{16a}$$

$$2\varepsilon_{xz}=\gamma^{(0)}{}_{xz}+z^2\gamma^{(2)}{}_{xz} \tag{16b}$$

Based on a higher-order nonlocal elasticity and strain gradient theory, the constitutive relations are:

$$\left(1-\mathcal{B}\nabla^2\right)\sigma^c{}_{xx}=\left(1-\ell^2\nabla^2\right)C_{xx}\varepsilon_{xx} \tag{17a}$$

$$\left(1-\mathcal{B}\nabla^2\right)\sigma^c{}_{xz}=\left(1-\ell^2\nabla^2\right)2C_{xz}\varepsilon_{xz} \tag{17b}$$

$$\left(1-\mathcal{B}\nabla^2\right)\sigma^p{}_{xx}=\left(1-\ell^2\nabla^2\right)\left(D_{xx}\varepsilon_{xx}-e_xE_z\right) \tag{18a}$$

$$\left(1-\mathcal{B}\nabla^2\right)\sigma^p{}_{xz}=\left(1-\ell^2\nabla^2\right)\left(2D_{xz}\varepsilon_{xz}-e_zE_x\right) \tag{18b}$$

$$\left(1-\mathcal{B}\nabla^2\right)D^p{}_x=\left(1-\ell^2\nabla^2\right)\left(2e_z\varepsilon_{xz}+\in_x E_x\right) \tag{18c}$$

$$\left(1-\mathcal{B}\nabla^2\right)D^p{}_z=\left(1-\ell^2\nabla^2\right)\left(e_x\varepsilon_{xx}+\in_z E_z\right) \tag{18d}$$

where $\mathcal{B} = (ea)^2$. $\sigma^c{}_{ij}$, $\sigma^p{}_{ij}$ and $D^p{}_i$ are nanobeam core stress tensor, piezoelectric face-sheets stress tensor and electric displacement component. Additionally, D_{ij} are elastic constants for piezoelectric layers, e_i are piezoelectric permittivity constants and $\in_i$ are dielectric permittivity constants.

5. EQUATIONS OF MOTION AND CLOSED-FORM SOLUTION PROCEDURE

Equations of motion are obtained based on modified Hamilton's variational principle including virtual strain energy U, virtual kinetic energy K, virtual electric field E, and virtual work done by external mechanical and electrical forces V in the form

$$\int_0^T \left(\partial U - \partial K - \partial E + \partial V\right) dt = 0 \tag{19}$$

A detailed explanation on the derivation of the equations of motion is presented in previous paper [64]. The equations of motion of FGM sandwich nanobeam are presented by displacements and obtained based on the nonlocal strain gradient theory as:

$$\begin{aligned} &A_{xx}^{(0)}\frac{\partial^2 u_0}{\partial x^2}+A_{xx}^{(1)}\frac{\partial^2 \varphi_x}{\partial x^2}-c_1A_{xx}^{(3)}\left(\frac{\partial^2 \varphi_x}{\partial x^2}+\frac{\partial^3 w_0}{\partial x^3}\right)+B_x^{(0)}\frac{\partial \Phi}{\partial x}-\ell^2\Bigg[A_{xx}^{(0)}\frac{\partial^4 u_0}{\partial x^4}+\\ &A_{xx}^{(1)}\frac{\partial^4 \varphi_x}{\partial x^4}-c_1A_{xx}^{(3)}\left(\frac{\partial^4 \varphi_x}{\partial x^4}+\frac{\partial^5 w_0}{\partial x^5}\right)+B_x^{(0)}\frac{\partial^3 \Phi}{\partial x^3}\Bigg]=I_0\ddot{u}_0-\mathcal{B}I_0\ddot{u}_0 \end{aligned} \tag{20a}$$

$$\begin{aligned} &-A_{xz}^{(0)}\left(\varphi_x+\frac{\partial w_0}{\partial x}\right)+2c_2A_{xz}^{(2)}\left(\varphi_x+\frac{\partial w_0}{\partial x}\right)-c^2{}_2A_{xz}^{(4)}\left(\varphi_x+\frac{\partial w_0}{\partial x}\right)+A_{xx}^{(1)}\frac{\partial^2 u_0}{\partial x^2}-\\ &c_1A_{xx}^{(3)}\frac{\partial^2 u_0}{\partial x^2}+A_{xx}^{(2)}\frac{\partial^2 \varphi_x}{\partial x^2}-c_1A_{xx}^{(4)}\frac{\partial^2 \varphi_x}{\partial x^2}-c_1A_{xx}^{(4)}\left(\frac{\partial^2 \varphi_x}{\partial x^2}+\frac{\partial^3 w_0}{\partial x^3}\right)+\\ &c^2{}_1A_{xx}^{(6)}\left(\frac{\partial^2 \varphi_x}{\partial x^2}+\frac{\partial^3 w_0}{\partial x^3}\right)+B_z^{(0)}\frac{\partial \Phi}{\partial x}+B_x^{(1)}\frac{\partial \Phi}{\partial x}-c_1B_x^{(3)}\frac{\partial \Phi}{\partial x}-c_2B_z^{(2)}\frac{\partial \Phi}{\partial x}-\\ &\ell^2\Bigg[-A_{xz}^{(0)}\left(\frac{\partial^2 \varphi_x}{\partial x^2}+\frac{\partial^3 w_0}{\partial x^3}\right)+2c_2A_{xz}^{(2)}\left(\frac{\partial^2 \varphi_x}{\partial x^2}+\frac{\partial^3 w_0}{\partial x^3}\right)-c^2{}_2A_{xz}^{(4)}\left(\frac{\partial^2 \varphi_x}{\partial x^2}+\frac{\partial^3 w_0}{\partial x^3}\right)+\\ &A_{xx}^{(1)}\frac{\partial^4 u_0}{\partial x^4}-c_1A_{xx}^{(3)}\frac{\partial^4 u_0}{\partial x^4}+A_{xx}^{(2)}\frac{\partial^4 \varphi_x}{\partial x^4}-c_1A_{xx}^{(4)}\frac{\partial^4 \varphi_x}{\partial x^4}-c_1A_{xx}^{(4)}\left(\frac{\partial^4 \varphi_x}{\partial x^4}+\frac{\partial^5 w_0}{\partial x^5}\right)+\\ &c^2{}_1A_{xx}^{(6)}\left(\frac{\partial^4 \varphi_x}{\partial x^4}+\frac{\partial^5 w_0}{\partial x^5}\right)+B_z^{(0)}\frac{\partial^3 \Phi}{\partial x^3}+B_x^{(1)}\frac{\partial^3 \Phi}{\partial x^3}-c_1B_x^{(3)}\frac{\partial^3 \Phi}{\partial x^3}-c_2B_z^{(2)}\frac{\partial^3 \Phi}{\partial x^3}\Bigg]=\\ &I_2\ddot{\varphi}_x-c_1I_4\left(2\ddot{\varphi}_x+\frac{\partial \ddot{w}_0}{\partial x}\right)+c^2{}_1I_6\left(\ddot{\varphi}_x+\frac{\partial \ddot{w}_0}{\partial x}\right)-\mathcal{B}\Bigg[I_2\frac{\partial^2 \ddot{\varphi}_x}{\partial x^2}-\\ &c_1I_4\left(2\frac{\partial^2 \ddot{\varphi}_x}{\partial x^2}+\frac{\partial^3 \ddot{w}_0}{\partial x^3}\right)+c^2{}_1I_6\left(\frac{\partial^2 \ddot{\varphi}_x}{\partial x^2}+\frac{\partial^3 \ddot{w}_0}{\partial x^3}\right)\Bigg] \end{aligned} \tag{20b}$$

$$
\begin{aligned}
&c_1 A_{xx}^{(3)} \frac{\partial^3 u_0}{\partial x^3} + A_{xz}^{(0)} \left(\frac{\partial \varphi_x}{\partial x} + \frac{\partial^2 w_0}{\partial x^2} \right) - 2c_2 A_{xz}^{(2)} \left(\frac{\partial \varphi_x}{\partial x} + \frac{\partial^2 w_0}{\partial x^2} \right) + c^2{}_2 A_{xz}^{(4)} \left(\frac{\partial \varphi_x}{\partial x} + \right. \\
&\left. \frac{\partial^2 w_0}{\partial x^2} \right) + c_1 A_{xx}^{(4)} \frac{\partial^3 \varphi_x}{\partial x^3} - c^2{}_1 A_{xx}^{(6)} \left(\frac{\partial^3 \varphi_x}{\partial x^3} + \frac{\partial^4 w_0}{\partial x^4} \right) - B_z^{(0)} \frac{\partial^2 \Phi}{\partial x^2} + c_2 B_z^{(2)} \frac{\partial^2 \Phi}{\partial x^2} + \\
&c_1 B_x^{(3)} \frac{\partial^2 \Phi}{\partial x^2} - \ell^2 \left[c_1 A_{xx}^{(3)} \frac{\partial^5 u_0}{\partial x^5} + A_{xz}^{(0)} \left(\frac{\partial^3 \varphi_x}{\partial x^3} + \frac{\partial^4 w_0}{\partial x^4} \right) - 2c_2 A_{xz}^{(2)} \left(\frac{\partial^3 \varphi_x}{\partial x^3} + \frac{\partial^4 w_0}{\partial x^4} \right) + \right. \\
&c^2{}_2 A_{xz}^{(4)} \left(\frac{\partial^3 \varphi_x}{\partial x^3} + \frac{\partial^4 w_0}{\partial x^4} \right) + c_1 A_{xx}^{(4)} \frac{\partial^5 \varphi_x}{\partial x^5} - c^2{}_1 A_{xx}^{(6)} \left(\frac{\partial^5 \varphi_x}{\partial x^4} + \frac{\partial^6 w_0}{\partial x^6} \right) - B_z^{(0)} \frac{\partial^4 \Phi}{\partial x^4} + \\
&\left. c_2 B_z^{(2)} \frac{\partial^4 \Phi}{\partial x^4} + c_1 B_x^{(3)} \frac{\partial^4 \Phi}{\partial x^4} \right] = I_0 \ddot{w}_0 + c_1 I_4 \frac{\partial \ddot{\varphi}_x}{\partial x} - c^2{}_1 I_6 \left(\frac{\partial \ddot{\varphi}_x}{\partial x} + \frac{\partial^2 \ddot{w}_0}{\partial x^2} \right) + \hat{N}_\varepsilon \frac{\partial^2 \ddot{w}_0}{\partial x^2} + \\
&\hat{N}_{xx} \frac{\partial^2 \ddot{w}_0}{\partial x^2} - \mathcal{B} \left[I_0 \frac{\partial^2 \ddot{w}_0}{\partial x^2} + c_1 I_4 \frac{\partial^3 \ddot{\varphi}_x}{\partial x^3} - c^2{}_1 I_6 \left(\frac{\partial^3 \varphi_x}{\partial x^3} + \frac{\partial^4 w_0}{\partial x^4} \right) + \right. \\
&\left. + \hat{N}_\varepsilon \frac{\partial^4 \ddot{w}_0}{\partial x^4} + \hat{N}_{xx} \frac{\partial^4 \ddot{w}_0}{\partial x^4} \right]
\end{aligned}
\tag{20c}
$$

$$
\begin{aligned}
&B_x^{(0)} \frac{\partial u_0}{\partial x} + B_x^{(1)} \frac{\partial \varphi_x}{\partial x} + B_z^{(0)} \left(\frac{\partial \varphi_x}{\partial x} + \frac{\partial^2 w_0}{\partial x^2} \right) - c_1 B_x^{(3)} \left(\frac{\partial \varphi_x}{\partial x} + \frac{\partial^2 w_0}{\partial x^2} \right) - \\
&c_2 B_z^{(2)} \left(\frac{\partial \varphi_x}{\partial x} + \frac{\partial^2 w_0}{\partial x^2} \right) - \mathscr{C}_z \Phi + \mathscr{C}_x \frac{\partial^2 \Phi}{\partial x^2} - \mathscr{C}_{x\phi} - \ell^2 \left[B_x^{(0)} \frac{\partial^3 u_0}{\partial x^3} + B_x^{(1)} \frac{\partial^3 \varphi_x}{\partial x^3} + \right. \\
&B_z^{(0)} \left(\frac{\partial^3 \varphi_x}{\partial x^3} + \frac{\partial^4 w_0}{\partial x^4} \right) - c_1 B_x^{(3)} \left(\frac{\partial^3 \varphi_x}{\partial x^3} + \frac{\partial^4 w_0}{\partial x^4} \right) - c_2 B_z^{(2)} \left(\frac{\partial^3 \varphi_x}{\partial x^3} + \frac{\partial^4 w_0}{\partial x^4} \right) - \\
&\left. \mathscr{C}_z \frac{\partial^2 \Phi}{\partial x^2} + \mathscr{C}_x \frac{\partial^4 \Phi}{\partial x^4} \right] = 0
\end{aligned}
\tag{20d}
$$

where $A_{ij}^{(m)}$, $B_j^{(m)}$, $\mathscr{C}_i$, $\mathscr{C}_{i\phi}$ and I_i stand for resultant stiffnesses, piezoelectric coefficients, dielectric coefficients and mass moments of inertias. The terms are also presented in [64].

For simply supported boundary conditions Navier solution method is used:

$$
\begin{pmatrix} u_0 \\ \varphi_x \\ w_0 \\ \Phi \end{pmatrix} = \sum_{n=1}^{\infty} \begin{pmatrix} \bar{u}_0 \cos(\beta_n x) e^{i\omega_n t} \\ \bar{\varphi}_x \cos(\beta_n x) e^{i\omega_n t} \\ \bar{w}_0 \sin(\beta_n x) e^{i\omega_n t} \\ \bar{\Phi} \sin(\beta_n x) e^{i\omega_n t} \end{pmatrix} \wedge \beta_n = \frac{n\pi}{L}
\tag{21}
$$

where $\bar{u}_0$, $\bar{\varphi}_x$, $\bar{w}_0$, $\bar{\Phi}$ are maximum values of displacements and electric potential. Natural frequency of the *n*th mode is expressed as ω_n.

System of governing equations are expressed in a vector form:

$$\left\{[K]-\omega_n[M]\right\}\left[\bar{u}_0 \quad \bar{\varphi}_x \quad \bar{w}_0 \quad \bar{\Phi}\right]^T = 0 \tag{22}$$

[*K*] and [*M*] are symmetric stiffness and inertia matrices, respectively. Components of these are presented in [64]. Presented solution procedure and numerical results based on it were comprehensively verified with results from the literature. Verification study is also presented in [64].

6. PARAMETRIC STUDY

The study ensures a novel perspective of analyzing small-scaled structures. The numerical results show the range of influences of nonlocal parameters on a dynamical response of complex nanobeam. To this aim, variation of length of the nanobeam with different nonlocal parameters values is considered to observe when size-dependent effects disappear for its vibration under in-plane electro-mechanical forces. The interaction range parameter is defined as differences in obtained solutions for classical (local) $\bar{\omega}^{l}_{n}$, and nonlocal $\bar{\omega}^{nl}_{n}$ theory of elasticity as:

$$\delta(\%) = \left| \frac{\bar{\omega}^{l}_{n} - \bar{\omega}^{nl}_{n}}{\bar{\omega}^{l}_{n}} \right| \cdot 100\% \tag{23}$$

The top lines are used to show dimensionless frequencies in form:

$$\bar{\omega}^{i}_{n} = \omega^{i}_{n} \cdot 10^2 \cdot L^2 \cdot \sqrt{\frac{I_0}{E_c I_2}} \quad for\ i = l, nl \tag{24}$$

where ω^{i}_{n} is dimensional frequency. The material and geometrical parameters of the studied sandwich nanobeam are assumed as follows h_p = 1.5 *nm*, h = 7 *nm*, ρ = 5550 *kg/m*^{3}, ρ_c = 3100 *kg/m*^{3}, ρ_m = 2700 *kg/m*^{3}, D_{xx} = 226 *GPa*, D_{xz} = 44.2 *GPa*, E_c = 380 *GPa*, E_m = 70 *GPa*, υ = 0.3, e_x = -2.2 *C/m*^{2}, e_z = 5.8 *C/m*^{2}, $\in_x = 5.64 \cdot 10^{-9}$ *C/Vm*, $\in_z = 6.35 \cdot 10^{-9}$ *C/Vm*. Not mentioned here coefficients are assumed to be variable and explained in individual studies.

What is more, the present section shows selected results for predicting nonlocal coefficients depending on expected free vibration frequencies, material gradation, distributions and volume of voids together with defined in-plane mechanical and electrical forces.

6.1 Nonlocal Interaction Range Parameter

Figure 3 displays influence of diverse length to thickness ratio on the nonlocal interaction range for fundamental frequency of the studied nanobeam with homogeneous (g = 0) core.

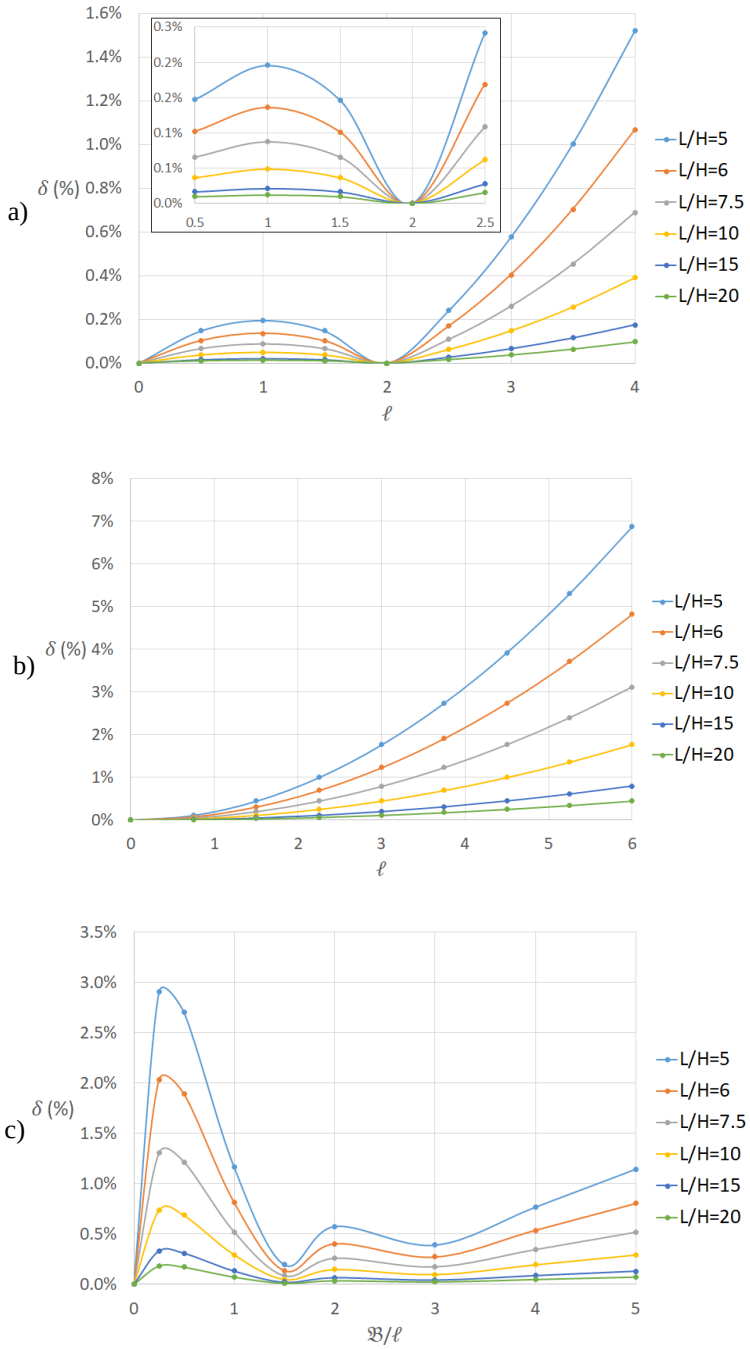

Fig. 3 Influence of length to thickness ratio on the nonlocal interaction range parameter for nanobeam fundamental frequencies: a) $\psi = 2$; b) $\mathcal{B} = 0$; c) pseudorandom ψ ratio

Nonlocal to length scale coefficients ratio is introduced as $\psi = \mathcal{B}/\ell$ and assumed for this study $\psi = 2$ *nm* in Fig. 3 a). Additionally, for Fig. 3b, it is assumed constant nonlocal coefficient of Eringen's elasticity as $\mathcal{B} = 0$ (pure Mindlin's strain gradient), and pseudorandom ψ ratio for Fig. 3c. The pseudorandom distribution was chosen to clearly present influence of nonlocal coefficients. Diverse ratios of nonlocal Eringen's to length scale coefficients are required in modelling nanostructures because values of nonlocal parameters vary due to initial stress, mode shape, rotary inertia, boundary conditions as well as material properties [69-72]. Based on Fig. 3, it may be concluded that the more lengthened the nanostructure is (higher length to thickness ratio), the lower impact of size-dependent parameters on dynamics of nanobeam. The scale coefficients refer to nanostructure and consequently has nanoscale dimensions. Therefore, large dimensions of the structure cause the effect of nanoscale to disappear. In the study, only length is used as a variable since nonlocal constitutive equations consider gradients of strains and stresses in the *x*-direction. For that reason, using thickness as a variable does not change mechanical response of the structure. On the other hand, increasing values of nano-scale coefficients induced higher gradients of stresses and strains (higher-order derivatives in equations of motion), and consequently, higher differences in results obtained by classical and nonlocal approaches. In addition, the study agrees with previous studies [58] that stiffness hardening and softening phenomena caused by strain and stress gradients disappear while $\ell^2 = \mathcal{B}$ because nonlocal parameters reduced each other out, consequently referring to classical elasticity. Moreover, greater differences are observed in the case of the strain gradient approach because only stiffness hardening effect is considered. Additionally, Fig. 3c clearly shows that appropriate detection of nonlocal parameters has a crucial role in predicting dynamic response of nano-scaled structures.

The effect of diverse axial in-plane forces on the nonlocal interaction range parameter for eigenfrequencies of homogeneous nanobeam is presented in Fig. 4. In the study, we assumed $\psi = 1.2$ *nm* and length of the nanostructure $L = 100$ *nm*. The study considers impact of both, mechanical forces and electrical loads induced by an external voltage. It should be noticed, applying compressive load (in both cases refer to positive values) relates to higher differences in classical- and nonlocal-based results. This is because additional compression generates strains and stresses in the structure. The nanostructure under compression experiences small shortening and bent. Thus, nonlocal parameters causing further gradients of stresses and strains result in greater differences between obtained results. The higher load is applied, the higher difference is achieved. It may be concluded that small-scale parameters have the most important role when the nanostructure is subjected to loads near their critical values. On the other hand, negative values of applied loads decrease the results differences because the tension causes opposite situation and results in a small lengthening of the structure.

Continuing study on diverse loads acting on sandwich nanobeam, the nonlocal interaction range parameter for natural frequency of nanobeam subjected to complex loadings is examined considering diverse length to thickness ratios. In the study, it is also assumed homogeneous core. Figure 5 indicates that despite simultaneous acting tension and compression, the applied loads lead to an increase of differences between results from local and nonlocal approaches. It is also observed, despite applying loads the nonlocal interaction range decrease with increasing length to thickness ratio. It clearly presents, increasing dimensions of the nanostructure decreases applications' range of size-dependent coefficients by decreasing a long-range interaction. Consequently, it may

be an important issue to appropriately detect the nonlocal parameters in terms of dimensions of the studied nanostructure.

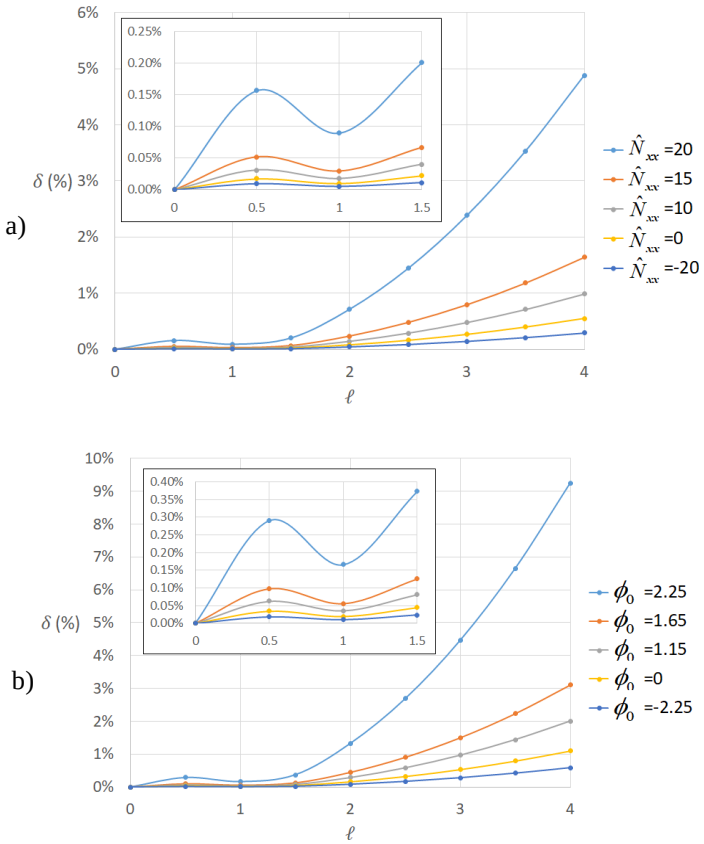

Fig. 4 Influence of external axial in-plane forces on the nonlocal interaction range parameter: a) mechanical forces; b) electrical forces

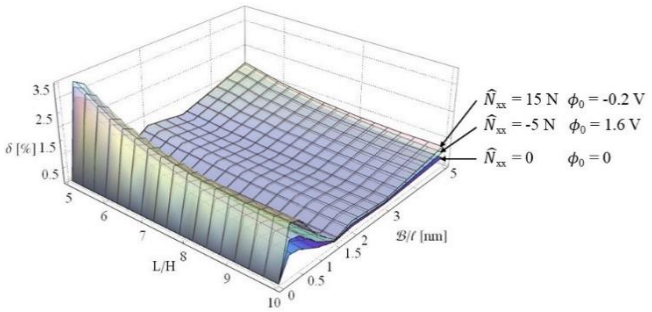

Fig. 5 Influence of complex loadings, length to thickness ratio and small-scale parameters on the nonlocal interaction range parameter

The effect of varying mechanical properties of functionally graded core in conjunction with nonlocal parameters and diverse length to thickness ratios on the nonlocal interaction range parameters is examined in Fig. 6. In this study, we assumed constant compressive force acting on the nanostructure as $\hat{N}_{xx} = 6$ *N*. According to previously discussed cases, size-dependent coefficients change influence on the nonlocal interaction range parameter depending on *L/H* ratios. Nevertheless, opposite to previous results, higher differences are observed for higher length to thickness ratio when the core structure is functionally graded. What is more, increasing the power-law index increases value of the nonlocal interaction range parameter. Varying material properties influence resultant stiffness and mass moments of inertias, consequently coupled with nonlocal parameters and higher-order displacements derivatives have a greater impact on a dynamic behavior of nanostructures. Moreover, applied compressive mechanical forces are approaching the critical value for FGM structure with *L/H* = 15. It confirms the previously stated suggestion that small-scale parameters are significant when the structure is under load that is near to its critical value.

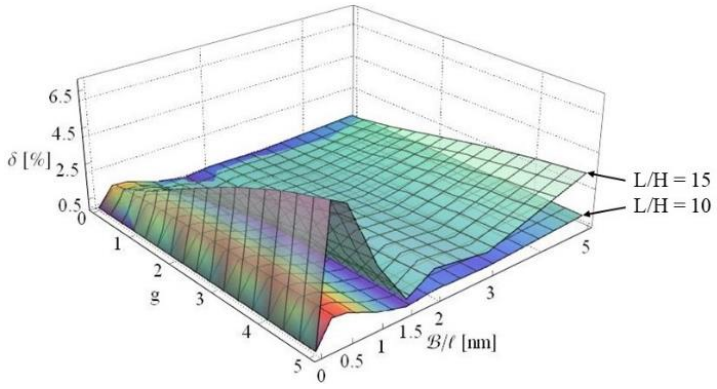

Fig. 6 Influence of length to thickness ratio, material gradation and small-scale parameters on nonlocal interaction range parameter

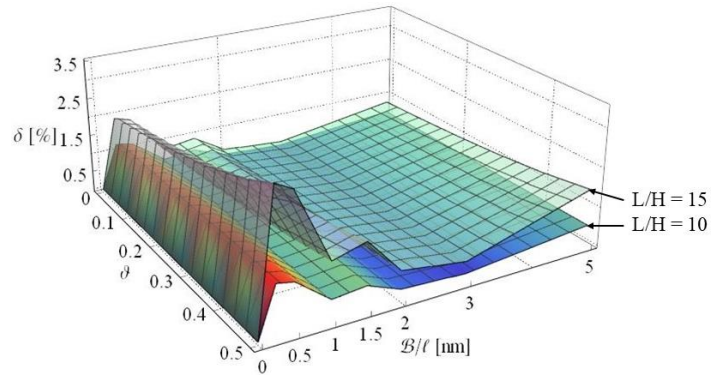

Fig. 7 Influence of length to thickness ratio, volume of voids and small-scale parameters on nonlocal interaction range parameter

Figure 7 displays impact of volume of voids (Type 1 porosity distribution), size-dependent parameters, and aspect ratio on the nonlocal interaction range parameter. In the study it is assumed that homogeneous nanobeam is subjected to electric field induced by external voltage $\phi_0 = 0.95\ V$. Similar to the previously discussed situation, increasing volume of voids decreases nanostructure's stiffness and mass density, so it affects resultant stiffness coefficients and mass moments of inertia. Therefore, applied nonlocal parameters and higher-order derivatives of displacements have a greater impact on free vibration response of nanobeam with lower stiffness and density. This investigation ensures, that regardless of mechanical or electrical forces are applied, loads tending to critical values have a higher impact on the nonlocal interaction range parameter because of more significant strains or stresses gradients.

The influence of diverse porosity distribution together with the porosity coefficient as well as length to thickness ratio is presented in Fig. 8. In the present study, homogeneous sandwich nanobeam is subjected to compressive mechanical forces $\hat{N}_{xx} = 15\ N$, and nonlocal parameters are assumed $\mathcal{B} = 1\ nm^2$ and $\ell = 4\ nm$. Diverse porosity types are characterized by different voids accumulation through the thickness of nanobeam core. Therefore, they have a diverse impact on resultant stiffness and density coefficients, and consequently, on the nonlocal interaction range parameter. Increasing volume of voids has a significant impact on the nonlocal interaction range parameter for higher values of length to thickness ratios. Weakness of the structure caused by porosity becomes important for structures with a high aspect ratio when the applied force is near the critical value. Therefore, regardless of whether the nanostructure stiffness is influenced by material gradation or porosity, the used size-dependent coefficients have a bigger impact on non-homogeneous structures. Thus, proper detection of nonlocal parameters is a significant issue, especially for heterogeneous structures.

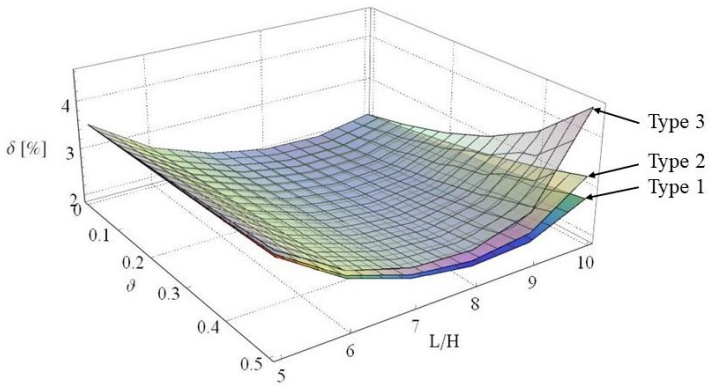

Fig. 8 Influence of diverse porosity distributions, volume of voids and length to thickness ratio on the nonlocal interaction range parameter

6.2 Detection of Nonlocal Parameters

In the current section, the detected values on nonlocal parameters are presented with superscripted *. First of all, Figure 9 presents predicted both Eringen's nonlocal coefficient and the length scale parameter for homogeneous and functionally graded

nanobeam. The figure shows the dependence of small-scale coefficients on assumed nanostructure's eigenfrequencies. It may be observed that increasing frequencies relate to decreasing Eringen's nonlocal constant. It agrees with the theory assumptions because the parameter is involved in stiffness softening phenomenon. So, the lower predicted frequencies are, the higher nonlocal coefficient is needed, because assuming constant other parameters, the structure must be softer. On the other hand, increasing length scale parameter causing stiffness hardening phenomenon, affects on increasing size-dependent parameter of Eringen. In contrast, increasing fundamental frequency values causes increasing in predicted length scale coefficient. Higher frequencies are related to stiffer construction (assuming constant mass) therefore higher length scale coefficient is required. Likewise, increasing Eringen's nonlocal parameter increases stiffness softening effect, so length scale parameter values are greater.

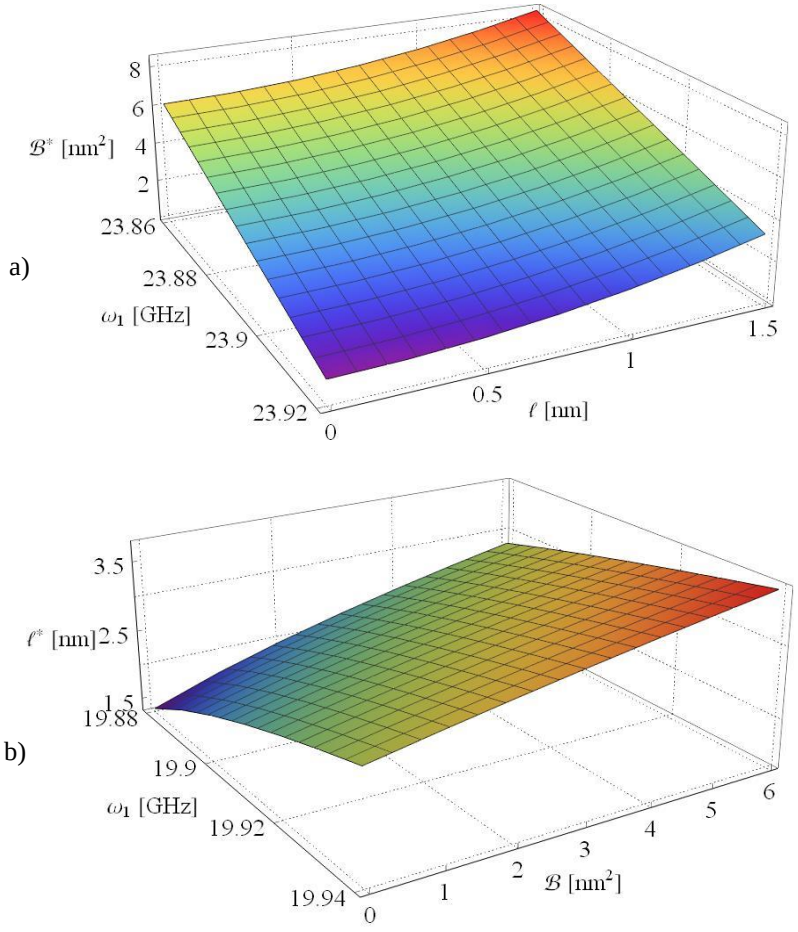

Fig. 9 Detection of nonlocal parameters for expected fundamental frequencies: a) Eringen's nonlocal coefficient for homogeneous nanobeam core; b) length scale parameter for FGM (g = 2) core

Next, relationship between nonlocal parameters and electro-mechanical forces is presented in Figure 10. In the study, we assumed $\psi = 4/3$ *nm* and expected fundamental frequency as $\omega_1 = 21.4$ *GHz* for homogeneous nanobeam. The structure is complexly loaded, so there are initial gradients of stress and strains. Increasing values of mechanical forces together with positive values of external voltage results in compression of the nanostructure. On the other hand, negative values of applied voltage refer to tension of the structure. Compression/tension of the structure results in its stiffness decrement/increment. Increasing values of nonlocal parameters involves a higher stiffness hardening effect due to assumed ratio of nonlocal to length scale coefficients. Therefore, increasing applied forces, with constant predicted nanobeam frequency, requires stiffness enhancement effect from nonlocal coefficients. Being knowledgeable about environment acting in NEMS device, for example, applied loads and operation's frequency, this solution gives a possibility to estimate/detect nanostructure nonlocal coefficients.

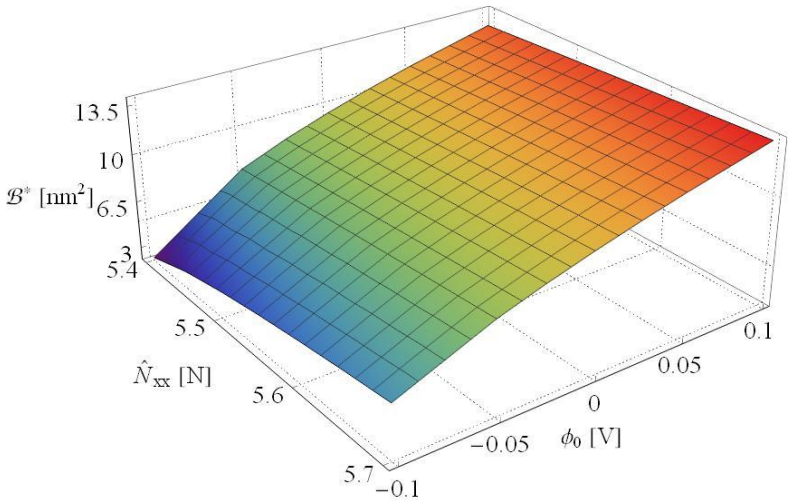

Fig. 10 Detection of nonlocal parameters for expected applied loads

Figure 11 represents a nonlocal parameters detection in view of porosity distributions and volume of voids. It is assumed homogeneous nanobeam core, nonlocal coefficients ratio as $\psi = 1.5$ *nm*, and fundamental frequency $\omega_1 = 24.65$ *GHz*. Increasing volume of voids decreases nanostructure stiffness and influences nanobeams mass. Nonetheless, diverse distribution affects stiffness and mass in diverse ways. Type 1 and 2 are characterized with non-porous bottom and lower surfaces, while Type 3 porosity distribution at these points is described with a maximum volume of porosity. Therefore, diverse effect on stiffness to mass ratios obtained from diverse porosity distribution is connected with diverse nano-scale effects from nonlocal coefficients.

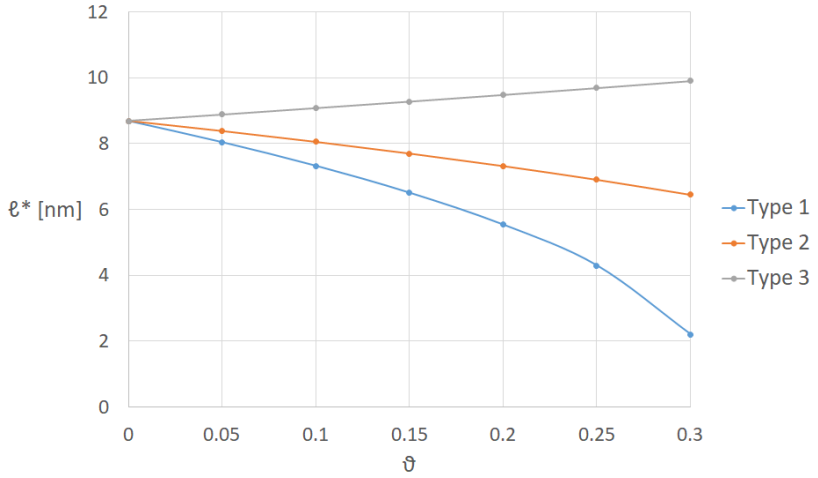

Fig. 11 Detection of nonlocal parameters for different porosity distributions and volume of voids

7. CONCLUDING REMARKS

The current study gives a different perspective to higher-order nonlocal strain gradient theory. The approach enables an analysis of differences in obtained results from classical and nonlocal theories for dynamic response of sandwich piezoelectric nanobeam under complex loads. The model represents a three-layered FGM porous beam-based nanoactuator subjected to external mechanical and electrical loads. Functionally graded material properties along with diverse porosity accumulation types are obtained based on the power-law distribution. The contribution of an electric field is represented by a combination of half-cosine and linear variation of the electric potential. Utilized equations of motion obtained based on Hamilton's principle and the nonlocal strain gradient theory, include Eringen's nonlocal coefficient and the length scale parameter to investigate both size-dependent phenomena from a single point of view. The displacement field is obtained based on Reddy third-order shear deformation theory that does not require shear correction factor, then it may be used for a wide range of structures. The results and discussion show effect of nonlocal parameters in conjunction with diverse length to thickness ratio, external loads, and material properties on a free vibration response of intelligent nanobeam.

Defined the nonlocal interaction range parameter clearly demonstrates that small-scale coefficients are dependent on geometrical properties of the structure, its material properties, and applied loads. Therefore, employing nonlocal theories is necessary for modelling of nanostructure-based ultra-small devices. What is more, the presented multi-parameter solution gives a possibility to estimate/detect nonlocal parameters for nanobeams based on assumed/predicted natural frequencies, material properties, and applied loads. Therefore, the conducted investigation, due to a widening understanding of nonlocal effects, may be an important tool in modelling, optimization, and control of NEMS devices.

Acknowledgement: *The paper has been conducted within WZ/WM-IIM/3/2020 project and was financed by the funds of the Ministry of Science and Higher Education, Poland.*

REFERENCES

1. Rieth, M., Schommers, W. (Ed.), 2005, *Handbook of Theoretical and Computational Nanotechnology*, American Scientific Publishers, USA.
2. Koochi, A., Abadyan, M., 2020, *Nonlinear Differential Equations in Micro/nano Mechanics*, Elsevier, Netherlands.
3. Maurya, D., Pramanick, A., Viehland, D. (Ed.), 2020, *Ferroelectric Materials for Energy Harvesting and Storage*, Elsevier, Netherlands.
4. Kamilla, S.K., Ojha, M., 2021, *Review on nano-electro-mechanical system devices*, Materials Today: Proceedings, in press, https://doi.org/10.1016/j.matpr.2021.02.801.
5. Lin, H., Zaeimbashi, M., Sun, N., Liang, X, Chen, H., Dong, C., Matyushov, A., Wang, X., Guo, Y., Sun, N.-X., 2018, *NEMS Magnetoelectric Antennas for Biomedical Application*, Proc. 2018 IEEE International Microwave Biomedical Conference (IMBioC).
6. Ilyas, S., Younis, M.I., 2020, *Resonator-based M/NEMS logic devices: Review of recent advances*, Sensors and Actuators A: Physical, 302, 111821.
7. Khazaai, J.J., Qu, H., 2012, *Electro-thermal MEMS switch with latching mechanism: design and characterization*, IEEE Sensors Journal, 12(9), pp. 2830–2838.
8. Ghayesh, M.H., Farajpour, A., 2019, *A review on the mechanics of functionally graded nanoscale and microscale structures*, International Journal of Engineering Science, 137, pp. 8-36.
9. Daikh, A.A., Houari, M.S.A., Eltaher, M.A., 2021, *A novel nonlocal strain gradient Quasi-3D bending analysis of sigmoid functionally graded sandwich nanoplates*, Composite Structures, 262, 113347.
10. Rapaport, D.C., 2004, *The art of Molecular Dynamics Simulations*, Cambridge University Press, Great Britain.
11. Farajpour, A., Ghayesh, M.H., Farokhi, H., 2018, A review on the mechanics of nanostructures, *International Journal of Engineering Science*, 133, pp. 231-263.
12. Toupin, R.A., 1962, *Elastic materials with couple-stresses*, Archive for Rational Mechanics and Analysis, 11, pp. 385-414.
13. Mindlin, R.D., Tiersten, H.F., 1962, *Effects of couple-stresses in linear elasticity*, Archive for Rational Mechanics and Analysis, 11, 415-448.
14. Koiter, W.T., 1964, *Couple stresses in the theory of elasticity*, I and II. Proceedings Series B, Koninklijke Nederlandse Akademie van Wetenschappen, 67, pp. 17-44.
15. Yang, F., Chong, A.C.M., Lam, D.C.C., Tong, P., 2002, *Couple stress based strain gradient theory for elasticity*, International Journal of Solids and Structures, 39(10), pp. 2731-2743.
16. Mindlin, R.D., 1964, *Micro-structure in linear elasticity*, Archive for Rational Mechanics and Analysis, 16, pp. 51–78.
17. Mindlin, R.D., 1965, *Second gradient of strain and surface-tension in linear elasticity*, International Journal of Solids and Structures, 1(4), pp. 417–438.
18. Lam, D.C.C., Yang, F., Chong, A.C.M., Wang, J., Tong, P., 2003, *Experiments and theory in strain gradient elasticity*, Journal of the Mechanics and Physics of Solids, 51, pp. 1477-1508.
19. Gurtin, M.E., Murdoch, A.I., 1975, *A continuum theory of elastic material surfaces*, Archive for Rational Mechanics and Analysis, 57, pp. 291-323.
20. Kroner, E., 1967, *Elasticity theory of materials with long range cohesive forces*, International Journal of Solids and Structures, 3, pp. 731-742.
21. Eringen, A.C., 1972, *Linear theory of nonlocal elasticity and dispersion of plane waves*, International Journal of Engineering Science, 10, pp. 425-435.
22. Eringen, A.C., 1972, *Nonlocal polar elastic continua*, International Journal of Engineering Science, 10, pp. 1-16.
23. Eringen, A.C., Edelen, D.G.B., 1972, *On nonlocal elasticity*, International Journal of Engineering Science, 10, pp. 233-248.
24. Eringen, A.C., 1983, *On differential equations of nonlocal elasticity and solutions of screw dislocation and surface wave*, Journal of Applied Physics, 54, pp. 4703-4710.
25. Romano, G., Barretta, R., 2017, *Nonlocal elasticity in nanobeams: the stress-driven integral model*. International Journal of Engineering Science, 115, pp. 14-27.
26. Lim, C.W., Zhang, G., Reddy, J.N., 2015, *A higher-order nonlocal elasticity and strain gradient theory and its applications in wave propagation*, Journal of the Mechanics and Physics of Solids, 78, pp. 298-313.

27. Chandel, V.S., Wang, G., Talha, M., 2020, *Advances in modelling and analysis of nano structures: a review*, Nanotechnology Reviews, 9(1), pp. 230-258.
28. Askes, H., Aifantis, E.C., 2009, *Gradient elasticity and flexural wave dispersion in carbon nanotubes*, Physical Review B, 80, 1995412.
29. Ouakad, H.M., Younis, M.I., 2010, *Nonlinear dynamics of electrically actuated carbon nanotube resonator*, Journal of Computational and Nonlinear Dynamics, 5, 011009.
30. Ke, L.-L., Wang, Y.-S., Yang, J., Kitipornchai, S., 2014, *Free vibration of size-dependent magneto-electro-elastic nanoplates based on the nonlocal theory*, Acta Mechanica Sinica, 30, pp. 516-525.
31. Mehralian, F., Beni, Y.T, 2017, *Thermo-electro-mechanical buckling analysis of cylindrical nanoshell on the basis of modified couple stress theory*, Journal of Mechanical Science and Technology, 31, pp. 1773-1787.
32. Lu, L., Guo, X., Zhao, J., 2017, *A unified nonlocal strain gradient model for nanobeams and the importance of higher order terms*, International Journal of Engineering Science, 119, pp. 265-277.
33. Ouakad, H.M., Sedighi, H.M., Al-Qahtani, H.M., 2020, *Forward and backward whirling of a spinning nanotube nano-rotor assuming gyroscopic effects*, Advances in Nano Research, 8, pp. 245-254.
34. Ouakad, H.M., Valipour, A., Żur, K.K., Sedighi, H.M., Reddy, J.N., 2020, *On the nonlinear vibration and static deflection problems of actuated hybrid nanotubes based on the stress-driven nonlocal integral elasticity*, Mechanics of Materials, 148, 103532,
35. Sedighi, H.M., Malikan, M., Valipour, A., Żur, K.K., 2020, *Nonlocal vibration of carbon/boron-nitridenano-hetero-structure in thermal and magnetic fields by means of nonlinear finite element method*, Journal of Computational Design and Engineering, 7(5), pp. 591-602.
36. Farajpour, A., Żur, K.K., Kim, J., Reddy, J.N., 2021, *Nonlinear frequency behaviour of magneto-electromechanical mass nanosensors using vibrating MEE nanoplates with multiple nanoparticles*, Composite Structures, 260, 113458.
37. Żur, K.K., Farajpour, A., Lim, C.W., Jankowski, P., 2021, *On the nonlinear dynamics of porous composite nanobeams connected with fullerenes*, Composite Structures, 274, 114356.
38. Hieu, D.V., Hoa N.T., Duy, L.Q., Thoa, N.T.K., 2021, *Nonlinear Vibration of an Electrostatically Actuated Functionally Graded Microbeam under Longitudinal Magnetic Field*, Journal of Applied and Computational Mechanics, 7, pp. 1537-1549.
39. Anjum, N., He, J-H., Ain, Q.T., Tian, D., 2021, *Li-He's Modified Homotopy Perturbation Method for Doubly-Clamped Electrically Actuated Microbeams-Based Microelectromechanical System*, Facta Universitatis, Series: Mechanical Engineering, 19(4), pp. 601-612.
40. Abouelregal, A.E., Mohammad-Sedighi, H., Faghidian, S.A., Shirazi A.H., *Temperature-Dependent Physical Characteristics of the Rotating Nonlocal Nanobeams Subject to a Varying Heat Source and a Dynamic Load*, Facta Universitatis, Series: Mechanical Engineering, 19(4), pp. 633-656.
41. Goharimanesh, M., Koochi, A., 2021, *Nonlinear Oscillationsof CNT Nano-resonator Based on Nonlocal Elasticity: The Energy Balance Method*, Reports in Mechanical Engineering, 2, pp. 41-50.
42. Wang, Q., Varadan, V.K, 2006, *Vibration of carbon nanotubes studied using nonlocal continuum mechanics*, Smart Materials and Structures, 15(2), pp. 659–666.
43. Reddy, J.N., 2007, *Nonlocal theories for bending, buckling and vibration of beams*, International Journal of Engineering Science, 45, pp. 288-307.
44. Wang, C.M., Zhang, Y.Y., He, X.Q, 2007, *Vibration of nonlocal Timoshenko beams*, Nanotechnology, 18(10), 105401.
45. Aydogdu, M., 2009, *Axial vibration of the nanorods with the nonlocal continuum rod model*, Physica E: Low-dimensional Systems and Nanostructures, 41, pp. 861-864.
46. Roque, C.M.C., Ferreira, A.J.M., Reddy, J.N., 2011, *Analysis of Timoshenko nanobeams with a nonlocal formulation and meshless method*, International Journal of Engineering Science, 49, pp. 976-984.
47. Li, C., Lim, C.W., Yu, J.L., Zeng, Q.C., 2011, *Analytical solutions for vibration of simply supported nonlocal nanobeams with an axial force*, International Journal of Structural Stability and Dynamics, 11(02), pp. 257–271.
48. Thai, H.T., 2012, *A nonlocal beam theory for bending, buckling, and vibration of nanobeams*, International Journal of Engineering Science, 52, pp. 56–64.
49. Thai, H.T., Vo, T.P., 2012, *A nonlocal sinusoidal shear deformation beam theory with application to bending, buckling, and vibration of nanobeams*, International Journal of Engineering Science, 54, pp. 58–66.
50. Ke, L.-L., Wang, Y.-S., Wang, Z.-D., 2012, *Nonlinear vibration of the piezoelectric nanobeams based on the nonlocal theory*, Composite Structures, 94, pp. 2038–2047.
51. Eltaher, M.A., Emam, S.A., Mahmoud, F.F., 2012, *Free vibration analysis of functionally graded size-dependent nanobeams*, Applied Mathematics and Computation, 218(14), pp. 7406–7420.
52. Berrabah, H.M., Tounsi, A., Semmah, A., Adda Bedia, E.A., 2013, *Comparison of various refined nonlocal beam theories for bending, vibration and buckling analysis of nanobeams*, Structural Engineering and Mechanics, 48(3), pp. 351–365.

53. Şimşek, M., 2014, *Large amplitude free vibration of nanobeams with various boundary conditions based on the nonlocal elasticity theory*, Composites Part B: Engineering, 56, pp. 621-628.
54. Rahmani, O., Pedram, O., 2014, *Analysis and modeling the size effect on vibration of functionally graded nanobeams based on nonlocal Timoshenko beam theory*, International Journal of Engineering Science, 77, pp. 55-70.
55. Nejad, M.Z., Hadi, A., 2016, *Non-local analysis of free vibration of bi-directional functionally graded Euler-Bernoulli nano-beams*, International Journal of Engineering Science, 105, pp. 1–11.
56. Beni, Y.T., 2016, *A Nonlinear Electro-Mechanical Analysis of Nanobeams Based on the Size-Dependent Piezoelectricity Theory*, Journal of Mechanics, 33, pp. 289–301.
57. Arefi, M., Zenkour, A.M., 2017, *Size-dependent vibration and bending analyses of the piezomagnetic three-layer nanobeams*, Applied Physics A, 123, 202.
58. Lu, L., Guo, X., Zhao, J., 2017, *Size-dependent vibration analysis of nanobeams based on the nonlocal strain gradient theory*, International Journal of Engineering Science, 116, pp. 12–24.
59. Liu, H., Liu, H., Yang, J., 2018, *Vibration of FG magneto-electro-viscoelastic porous nanobeams on visco-Pasternak foundation*, Composites Part B: Engineering, 155, pp. 244–256.
60. Thai, S., Thai, H.T., Vo, T.P., Patel, V.I., 2018, *A simple shear deformation theory for nonlocal beams*, Composite Structures, 183, pp. 262–270.
61. Karami, B., Janghorban, M., 2019, *A new size-dependent shear deformation theory for free vibration analysis of functionally graded/anisotropic nanobeams*, Thin-Walled Structures, 143, 106227.
62. Liu, H., Lv, Z., Wu, H., 2019, *Nonlinear free vibration of geometrically imperfect functionally graded sandwich nanobeams based on nonlocal strain gradient theory*, Composite Structures, 214, pp. 47–61.
63. Jankowski, P., Żur, K.K., Kim, J., Reddy, J.N., 2020, *On the bifurcation buckling and vibration of porous nanobeams*, Composite Structures, 250, 112632.
64. Jankowski, P., Żur, K.K., Farajpour, A., 2022, *Analytical and meshless DQM approaches to free vibration analysis of symmetric FGM porous nanobeams with piezoelectric effect*, Engineering Analysis with Boundary Elements, 136, pp. 266-289.
65. Nasr, M.E., Abouelregal, A.E., Soleiman, A., Khalil, K.M., 2021, *Thermoelastic Vibrations of Nonlocal Nanobeams Resting on a Pasternak Foundation via DPL Model*, Journal of Applied and Computational Mechanics, 7, pp. 34-44.
66. Abdelrahman, A.A., Esen, I., Özarpa, C., Eltaher, M.A., 2021, *Dynamics of perforated nanobeams subject to moving mass using the nonlocal strain gradient theory*, Applied Mathematical Modelling, 96, pp. 215–235.
67. Wang, Q., 2002, *On buckling of column structures with a pair of piezoelectric layers*, Engineering Structures, 24, pp. 199-205.
68. Reddy, J.N., 2007, *Energy principles and variational methods in applied mechanics*, John Wiley & Sons, USA.
69. Thai, H.T., Vo, T.P., Nguyen, T.K., Kim, S.E., 2017, *A review of continuum mechanics models for size-dependent analysis of beams and plates*, Composite Structures, 177, pp. 196-219
70. Ghavanloo, E., Fazelzadeh S.A., 2016, *Evaluation of nonlocal parameter for single-walled carbon nanotubes with arbitrary chirality*, Meccanica, 51, pp. 41-54.
71. Zhang, Z., Wang, C.M., Challamel, N., 2014, *Eringen's length scale coefficient for buckling of nonlocal rectangular plates from microstructured beam-grid model*, International Journal of Solids and Structures, 51, pp. 4307-4315.
72. Mehralian, F., Beni, Y.T., Zeverdejani, M.K., 2017, *Calibration of nonlocal strain gradient shell model for buckling analysis of nanotubes using molecular dynamics simulations*, Physica B: Condensed Matter, 521, pp. 102-111.